View metadata, citation and similar papers at core.ac.uk
brought to you by CORE
provided by Apollo

Integrated, portable, tunable, and coherent terahertz sources and sensitive detectors based on layered superconductors

Kaveh Delfanazari, *Senior Member, IEEE*, Richard A. Klemm, *Member, IEEE*, Hannah J. Joyce, *Member, IEEE*, David A. Ritchie, Kazuo Kadowaki, *Member, IEEE*

***Abstract*—At terahertz (THz) frequencies, between 0.1-10 THz, current compact emitter and receiver technologies are generally inefficient and impractical. Hence, a gap exists between mature microwave and developed optical technologies. On-chip, integrated broadly tunable and powerful quantum sources that coherently radiate THz waves between 0.1 and 11 THz (potentially extendable to 15 THz) and with potential output power of > 1 mW can be achieved based on quantum tunneling of electron pairs across the stack of intrinsic Josephson junctions (IJJs) naturally present in a single crystal of the layered high-T_c superconducting $Bi_2Sr_2CaCu_2O_{8+\delta}$ (BSCCO). Such devices have been found to be especially promising solid-state THz sources capable of bridging the entire THz gap, as their wide frequency tunability range is superior to that obtained from their semiconducting based rivals, either single resonant tunneling diodes (RTDs) or THz-quantum cascade lasers (QCLs). Due to the unique electrodynamics of BSCCO, they can also be operated as switching current detectors, paving the way for the realization of on-chip THz integrated circuits for applications in ultrahigh-speed telecommunications, quantum information, on-chip spectroscopy, and non-destructive sensing, testing, and imaging. This paper reviews the history and recent advances in THz sources and detectors based on IJJs with a focus on the application of IJJ THz devices in THz spectroscopy, and various types of THz imaging systems such as r**

eflection, transmission, and computed tomography. We show that compact IJJ THz devices with sub-centimeter-sized modules are easy to use in many applications, as they can be regarded as pocket quantum THz torches.

***Index Terms*—** THz waves, cavity modes, intrinsic Josephson junctions, Josephson plasmonic, THz integrated circuits, layered superconductors, quantum emitters, solid-state light sources, and detectors.

I. Introduction

THE frequencies *f* between microwaves (MW) and infrared (IR), in the electromagnetic (EM) spectrum are often called terahertz (THz, 1 THz = 10^{12} c/s) band. This band (*f*= 100 GHz-10 THz) has received considerable attention because it contains the vibrational frequencies of several categories of molecules and materials [1,2]. Furthermore, THz technology has become significant in the fields of quantum information processing, high-speed communication, indoor and space wireless telecommunications, medicine and medical diagnostics, pharmaceutical, biotechnology, bio-sciences, non-destructive imaging, sensing, and testing, etc. Thus, interest in THz science and technology grows rapidly [1-3].

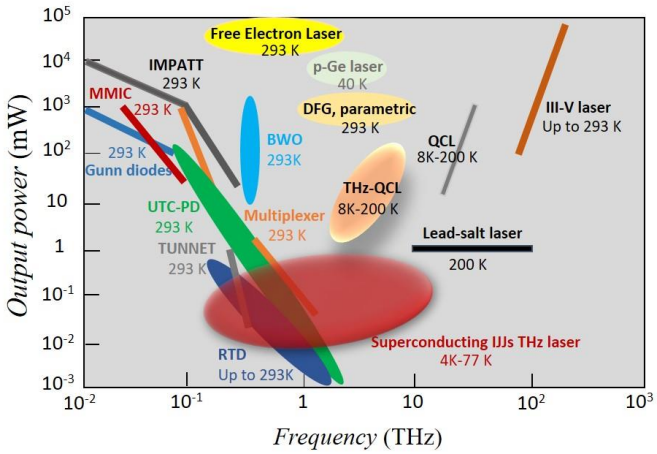

Fig. 1: A diagram summarizing the available THz sources with their output power, operating frequency and temperatures. Continuous waves (CW) IJJ THz laser discussed in this paper covers the entire THz gap: frequencies from 0.1 to 11 THz with THz power of up to 0.6 mW through its present operating circuitry (see the red ellipse in the figure).

Among artificial THz sources of large scale, with the cavity dimensions of > mm^2, there are several types to date, such as gyrotron [4], backward wave oscillators (BWO) or carcinotron [5], far infrared laser (FIR-laser) [1], free-electron lasers (FEL) [6], synchrotron light sources [7], photomixers [8], photoconductive antennas [9], photo-Dember emitters [10], optical rectifiers [2], uni-traveling carrier photodiodes [11], impact ionization avalanche transit-time (IMPATT) diodes [12], microwave monolithic integrated circuits (MMIC) [13],

K. Delfanazari (corresponding author) is with the Electrical Engineering Division, Department of Engineering, and the Department of Physics, Cavendish Laboratory, University of Cambridge, Cambridge, UK (e-mail: kd398@cam.ac.uk).

R. A. Klemm is with the Department of Physics, University of Central Florida, Orlando, FL, USA.

H. J. Joyce is with the Electrical Engineering Division, Department of Engineering, University of Cambridge, Cambridge, UK.

D. A. Ritchie is with the Department of Physics, Cavendish Laboratory, University of Cambridge, Cambridge, UK.

K. Kadowaki is with the Graduate School of Pure and Applied Sciences, & Algae-Biomass and Energy System (ABES) Research and Development Center, University of Tsukuba, Tsukuba, Ibaraki, Japan.

tunnel injection transit time (TUNNEtT) [2], Schottky barrier diodes (SBDs) [2], and nonlinear frequency-mixing generation [14]. Resonant tunneling diodes (RTDs) [15,16], quantum cascade lasers (QCLs) [17-19], and intracavity difference frequency generation in QCLs [20,21] fall in the category of compact solid-state THz sources with cavity dimensions of < mm^2.

Figure 1 provides further information about the present available THz sources with their operation power, temperature, and frequency range. As THz pulse detectors, photoconductive antennas based on low-temperature-grown GaAs, or electro-optic sampling techniques are often used. As continuous-wave THz detectors, silicon (Si) and indium antimonide (InSb) based hot-electron bolometers, SBDs, superconductor–insulator–superconductor (SIS) junctions, and superconducting tunnel junctions coupled to a thin superconducting film are widely used [2].

Here, we discuss a new generation of solid-state devices with inherently small power dissipation (due to superconductivity) that is compact, portable, and continuous THz sources based upon the intrinsic Josephson junctions (IJJs) in the layered high transition temperature (T_c) superconductor, $Bi_2Sr_2CaCu_2O_{8+\delta}$ (BSCCO). Due to the unique electrodynamics of BSCCO, it allows for the manufacture of sensitive and efficient THz detectors such as switching current THz detectors. As shown by the red ellipse in Fig. 1, the frequency range and power that such THz devices (with cavity dimensions of less than 100 × 500 μm^2) can cover are broad, paving the way for the realization of on-chip THz integrated circuits for various applications.

II. THz Generation and Detection in Layered BSCCO

The *ac*-Josephson effect [22] intrinsic to atomic-scale layered superconducting BSCCO [23,24] can provide the possibility of generating and detecting THz waves in a broadly tunable frequency range.

A. Coherent and Continuous-wave IJJ THz sources

BSCCO has the perovskite structure and comprises a one-dimensional stack of alternating superconducting (below T_c) CuO_2 double layers and insulating Bi_2O_2 layers, which together form the IJJs [24,25]. Therefore, BSCCO is such an extremely anisotropic layered superconductor and regarded as a stack of identical IJJs. Each of the naturally identical junctions is 1.533 nm thick, and they are evenly spaced with two junctions per unit cell *c*-axis edge length.

Coherent and continuous EM waves with frequencies ranging between f= 0.3 GHz and 11 THz (and potentially up to 15 THz) can be generated in BSCCO by applying a *dc*-voltage V across the active IJJs, due to the *ac*-Josephson current. The emitted THz wave frequency satisfies the *ac*-Josephson relation, $f = f_J = (2e/h)\, V/N$, = 0.483597891 THz for V/N= 1 mV. Here, e is the electric charge, h is Planck's constant, and N is the number of active junctions. Consequently, the set of IJJs is regarded as a natural voltage to frequency transducer.

Due to strong anisotropy BSCCO behaves as an insulator for electric fields parallel to its *c*-axis ($E \| \hat{c}$). The three-dimensional mesa structure fabricated using single-crystalline BSCCO also behaves as an internal EM cavity, which typically couples to the non-linear *ac*-Josephson currents radiated in IJJs.

The mechanism of THz emission from BSCCO IJJs is found to be (i) the *ac*-Josephson effect and electric dipole radiation owing to the uniform term of the *ac*-Josephson current along the *c*-axis, as well as (ii) the cavity resonance condition characterized by the cavity size and shape. Intense radiation occurs when there is strong coupling between (i) and (ii) at one or more transverse magnetic cavity mode frequencies. The weak coupling results in broadband THz radiation, which is tunable over a wide frequency range [20,21].

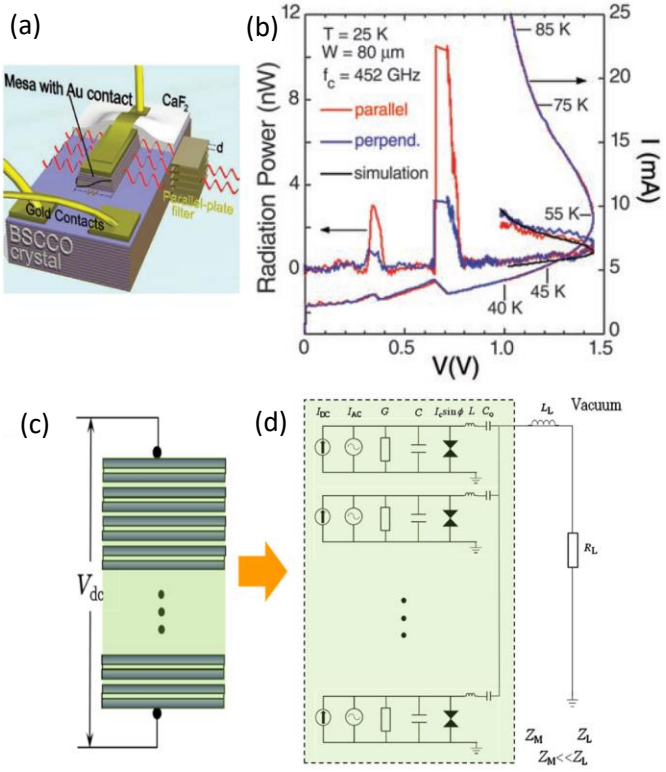

Fig. 2: Schematic diagram of the BSCCO IJJ THz source (a). The applied *c*-axis current stimulates the fundamental cavity mode (solid half-wave) on the width w of the rectangular cavity, and EM waves at THz frequencies are emitted from the side faces (red waves) [26]. Current-voltage characteristics (IVCs) and THz power of the THz cavity with a width of 80 μm. See text for more detail [26]. The schematic of the BSCCO IJJ THz source (c) and its equivalent circuit diagram (d) [30].

The first experimental observation of the EM wave radiation from BSCCO, with a broad linewidth due to out of phase radiation, was reported by Kleiner *et al.* [25, 28]. Later, Batov *et al.* reported the observation of EM waves in the THz region (at a frequency up to 0.5 THz with a radiation power of ~ pW) by fabricating as many as 100 junctions in a step-like geometry [29].

Figure 2 (a-b) shows the results of the first demonstration of a BSCCO THz emitter in the form of a mesa with width, length, and height of 80 μm, 300 μm, and 1 μm, respectively [26]. The device was fabricated by thermal evaporation, photolithography, and Ar ion milling techniques [26,27]. The IVCs and the radiation power detected by the bolometer can be

seen in Fig. 2(b) [26]. Two radiation peaks were detected near V= 0.37 V, and 0.71 V that were attributed to Josephson- (former) and thermal- (latter) radiations with a total radiation power of ~0.5 μW. This record output power observed was more than 10^4 times larger than in previous reports.

Subsequently, IJJ THz devices of different cavity shapes and dimensions were experimentally and theoretically studied. It was found that almost in all cases, the radiation is coherently synchronized in the stack of IJJs. This was evidenced by the fact that the detected THz power from N IJJs, was found to be proportional to N^2 indicating that all radiating IJJs are coherently generating THz waves [30-72].

(i) Equivalent circuit of IJJ THz emitters

To estimate the maximum output power from IJJ THz emitters, their schematic (c) and equivalent circuit (d) illustrations are shown in Fig. 2 [30]. A maximum output power P_{max} ($\approx I_c^2 Z_L/8$) from a source with output impedance Z_M can be observed if the condition $Z_M \approx Z_L$ is fulfilled (impedance matching with a load where Z_L = 377 Ω is the impedance of vacuum). Here, I_c is the c-axis critical current of the mesa. For a typical current I_c ~20 mA, a $P_{max} \approx$ 20 mW can easily be achieved with the current device architecture. One advantage of such IJJs THz devices over devices made from conventional JJs is that, in contrast to the latter, the impedance mismatching is adjusted naturally by the effective shunt mechanism for the c-axis resistance of the mesa (it is always around 100 Ω, regardless of the base temperature) due to the inhomogeneous heating [30].

(ii) The narrow intrinsic linewidth of IJJ THz sources

The intrinsic radiation linewidths of the IJJ THz sources are very narrow, and generally far below the resolution of Fourier transform infrared (FT-IR) spectrometer which is between 7-12 GHz, depending upon the equipment used. Frequency heterodyne mixing experiments at low temperatures determined the linewidth to be 500 MHz at low-current I bias regime, but at high I bias, another experiment showed that the intrinsic linewidth could be as small as 23 MHz (see Fig. 3(a)) [31,32]. A narrow emission linewidth as low as 6 MHz with central emission frequency of 445 GHz at T= 45 K has also been observed recently [32]. As shown in Fig. 3 (b), the radiation linewidth is strongly temperature-dependent and decreases approximately as $\Delta f \approx T_b^{-4}$. For all THz mesa type devices, the emission linewidth also decreases inversely with the number of phase-locked JJs (N).

(iii) Emission Tunability of the IJJ THz sources

BSCCO, with a superconducting gap of magnitude above 60 meV, will potentially allow frequency f to be tunable up to 15 THz [30-72]. The tunability has first been improved in two different approaches: (1) by modification of boundary conditions in mesa cavities and changing the cavity dimensions, using focused ion beam (FIB) milling or other milling techniques (a discrete frequency tuning can be obtained) and by probing the radiation emitted from the outer or inner IVC branches when the bias voltage is changed (for a continuous frequency tuning).

For instance, Fig. 4 (a) shows the tunable radiation between 0.495 THz and 0.934 THz generated from an acute isosceles triangular cavity. This record 47% tunability reported by Delfanazari *et. al.* was the broadest range of frequencies detected from the outer-most IVCs (where an equal bias is distributed across all IJJs in the cavity) of mesa devices of any geometry [33]. Most detected THz frequencies could only be linked to the *ac*-Josephson effect and the cavity resonance contribution in enhancing the radiation was minimum.

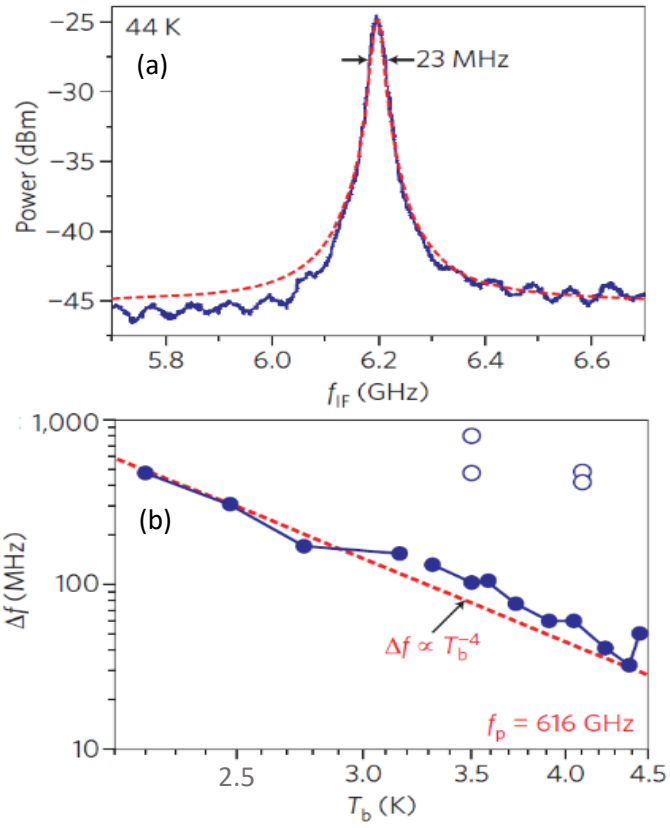

Fig. 3. (a) the emission linewidth measured at T= 44 K and in high-bias regime of the IVCs [32]. A fit to a Lorentzian line profile is shown with red dashed line. (b) solid and open symbols are the temperature dependence of the linewidth in the high- and low-bias regime, respectively. The red line shows a fit $\Delta f \approx T_b^{-4}$, where T_b is the cryostat temperature. The linewidth in the low-bias regime is around a factor of ten larger than that in the high-bias regime [32].

In a different approach, Tsujimoto *et. al.* examined the inner IVCs branches (where a part of IJJs is still in the resistive state) of the rectangular mesas. This was motivated by the fact that the reduced effective number of IJJs (N) in the inner branches results in higher frequencies at a fixed voltage (second Josephson relation). THz radiation with emission over a broad frequency range was discovered in internal IVC branches by varying the bias voltage [35].

There have been recent reports of broadly tunable THz radiation achieved by further development in the design and fabrication of the THz cavities. Kashiwagi *et. al.* reported the observation of the tunable emission (up to 2.4 THz) from stand-alone disk-shape cavities [64]. From the small but thick mesas, Borodianskyi *et. al.* observed THz radiation with a record

frequency tunability observation of 1 to 11 THz, see Fig. 4 (b), with a good efficiency [65]. The high end of this extremely tunable THz radiation is near to the edge of the BSCCO superconducting energy gap. Such emission can be observed if the threshold number of junctions $N > 100$ is fulfilled. In this case, similar to that in QCLs, the cascade amplification of the photon number occurs as all IJJs collectively pump the synchronized cavity modes. This means that IJJ devices have a laser-like threshold.

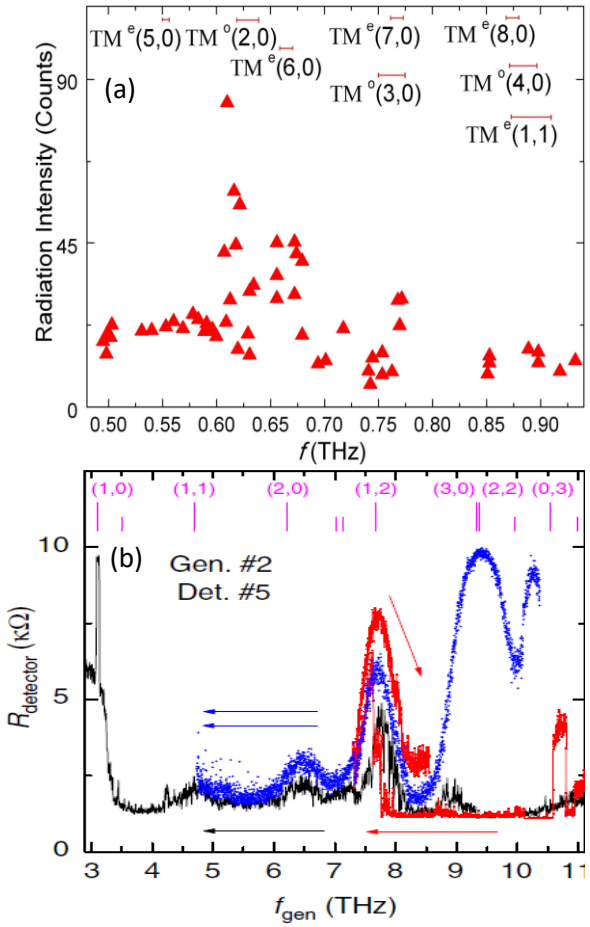

Fig. 4. (a) the overall radiation intensity of the acute isosceles triangular THz emitter between temperatures $T = 10$ and 50 K versus frequency. The corresponding cavity mode frequencies are listed at the top [33]. (b) The emission spectra: detector response vs. Josephson frequency. Different sweeps are shown by different colors. Sweeping directions are shown by arrows. Expected positions of primary cavity modes are shown by bars at the top [65].

They reported the emission frequency range for two different THz sources, both of which are very broad: 3–11 THz for one device and 1–9 THz for another one. Like all previous studies, these devices also show continuous THz emission radiated in the entire range of frequencies. The strongest THz emission was attained when one of the cavity resonance frequencies and the Josephson frequency matched.

The broadly tunable THz emitters reported by Borodianskyi *et. al.* based on superconducting BSCCO are superior to solid-state THz emitters of any other type, including semiconducting lasers such as QCLs and RTDs [3,16,65]. Thus, superconducting THz sources are one of the most promising compact devices capable of bridging the THz gap.

(iv) Powerful IJJ THz sources

For IJJ THz sources to be used in various THz applications, their THz power P must be in excess of 1 mW. There have been many efforts in different ways to improve the output P of these THz sources. The maximum P reported from a single device of any cavity shape such as conventional mesa structures (with a thin superconducting substrate) [30-70] or stand-alone mesas (without a superconducting substrate) [44,64] ranges between 30 and 110 μW. Here, we discuss some different approaches that have been performed for P enhancement of IJJ THz sources:

(iv-I) Fabrication of an array of IJJ THz emitters

By synchronization of the THz radiation from parallel arrays of rectangular IJJ THz sources on a single chip, Orita *et al.* experimentally demonstrated THz frequency locking from neighboring cavities onto one f value. This was associated with an increase in THz P characteristic of total coherence [56].

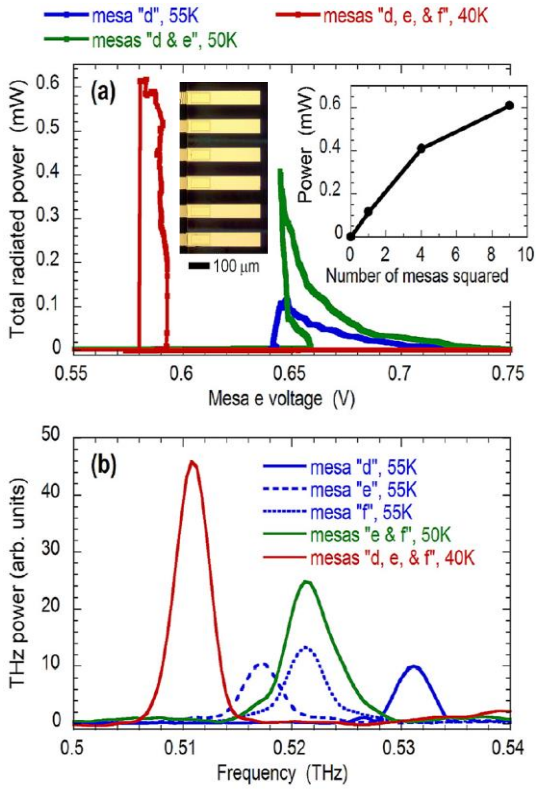

Fig. 5. (a) THz power vs. bias voltage at optimized bath temperature for one (blue curve), two (green curve), and three (red curve) mesa cavities. Inset shows the measured maximum THz power as approximate square of number of devices. The optical micrograph of array of mesas with dimensions of 400 × 600 μm^2. (b). Spectra at maximum THz power for one (blue), two (green), and three (red) mesas [66].

To overcome the limit on the viable number of IJJs in a cavity which directly relates to the control of heat through the base of the mesas, Benseman *et al.* later reported the experimental observation of a record $P \sim 610$ μW at $f = 0.51$ THz, by phase synchronizing the radiation from three conventional mesa arrays [56]. This was an important step towards the

development of high-powered IJJ THz emitters.

From the synchronization of two mesa arrays (one with eight and the other with six parallel mesas-see inset of Fig. 5 (a), they found that P scales as the square of the number of biased devices, provided that at the cavity resonance frequency, all cavities are within one free-space wavelength (in the present experiment up to four devices).

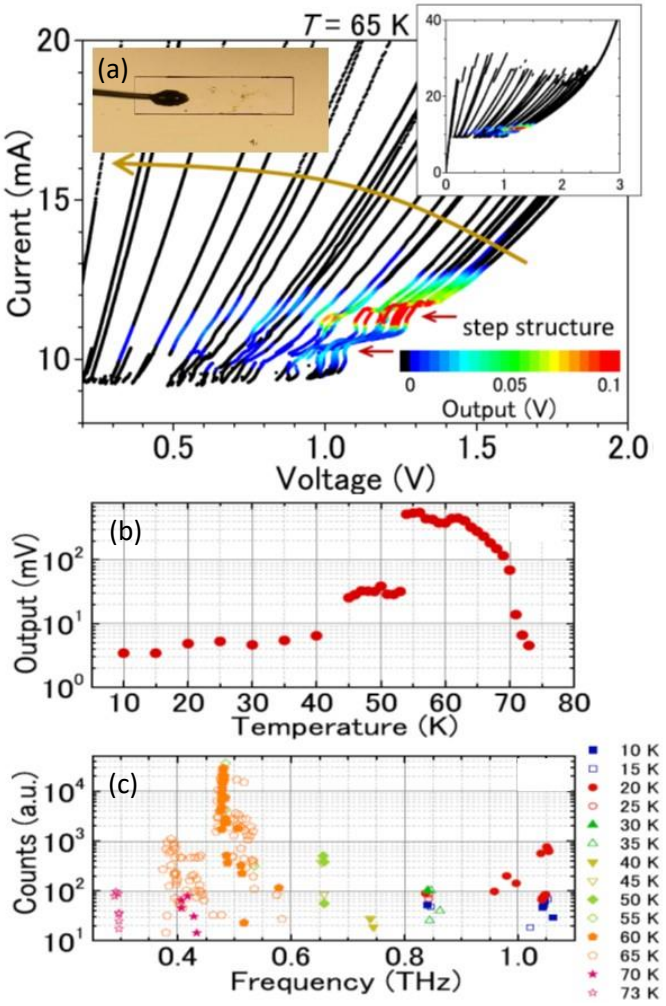

Fig. 6: (a) inset in the left: an optical micrograph of a stand-alone rectangular THz antenna [67]. The inner branches in IVCs of a stand-alone mesa. Right inset at Fig. 6 (a) is the overall multi-branched IVCs for 65K. Emission intensity of a single stand-alone device versus temperature (b) and frequency (c) [67].

However, for larger arrays, P scales linearly with the number of devices. Phase synchronization among adjacent devices was attained by EM coupling over the bulk of the BSCCO. This is because in the case of radiating mesas, there is radiation leakage into the base BSCCO. The leakage radiation also comprises the same in-plane wavevector as the cavities, so for THz devices spaced at w, an efficient synchronized coupling could be observed.

With the mesa cavity design of their study, the maximum observable THz power vs. bias voltage of one device usually peaked around 120 μW, for bath temperatures between T= 40K and 55 K. When they biased three devices on a chip at a time, they found a P of up to 610 μW (inset in Fig. 5 (a). They also found that the strongest radiation arises at a somewhat higher temperature than for individual devices and correspondingly lower voltages (Fig. 5 (a)) and emission frequency (Fig. 5 (b)). They could not manage mesa arrays with more than three synchronized devices on a chip, as the total power dissipation became excessive, so it was not possible to keep the devices cold enough to operate optimally.

(iv-II) Tunable and powerful stand-alone THz sources

In IJJ THz emitters, the strong Joule heating (due to poor thermal conductivity of the BSCCO substrate) led to back-bending in the IVCs of the devices, limiting the application of large V to the devices, which is necessary for powerful THz output. To overcome this heating issue or at least to get better IVCs, a new type of device, stand-alone mesas, cleaved from the BSCCO substrate, and with Au films deposited on their tops and bottoms, were first proposed [59,60] and then realized [35,36,67]. This structure greatly improves the thermal behavior of the IJJ THz devices. With such stand-alone devices, the possible applied bias V and the corresponding IVC loop could be in principle increased to over 5 V, which would be three times the highest achieved values in conventional IJJ THz devices with a BSCCO substrate.

Here, as an example, we discuss the powerful and tunable stand-alone THz sources reported by Kitamura *et al.* [67]. The left inset in Fig. 6 (a) shows the rectangular stand-alone THz cavity with top/bottom widths w= 74/84 μm, length l= 280 μm, and thickness t= 1.9 μm. In Fig. 6 (a), a remarkable step structure in the inner IVCs branches can be seen. The radiation power P gradually decreases by sweeping the IVC from right to left, with the number N of IJJs (see the yellow curved arrow). This weakening behavior of P can be attributed to $P \propto N^2$ [26].

Figure 6 (b) shows the temperature T dependence of the THz power recorded by the Si-bolometer for T= 10 K and 73 K-which was attained only from the low I bias region. It is seen that by increasing T from the lowest bath temperature up to BSCCO T_c, the outermost IVC branch THz radiation power also rises. There is a jump at T= 54 K, with a peak at 56 K. The radiation then weakens abruptly above T= 70 K and vanishes at T= 74 K. Sekimoto *et al.* also reported similar results from both high and low I bias areas [67]. Figure 6 (b) is the temperature dependence THz frequencies measured by the FT-IR, which shows a sharp intensity peak due to the cavity resonance effect.

It is remarkable to find such broadly tunable THz radiation with a minimum at f of 0.29 THz (at T= 73 K), and a maximum at f of 1.06 THz (at T= 10 K) from a single device. They attributed the observed peak of the THz power (from f= 0.47 - 0.49 THz, with $P \approx 20$ μW) to the fundamental TM (1,0) mode frequency f = 0.483 THz. Moreover, the relatively weak emission appeared at f= 1.05 THz was found to be the fundamental TM (2,0) mode at $f^c_{2,0}$.

In further investigations on such devices, Kashiwagi *et al.* reported a cylindrical stand-alone IJJ THz emitter that was tunable from 0.5 to the record 2.4 THz within a single device. Such broadly tunable THz emission was observed just by changing the device operating temperature and the voltage bias

across the THz cavity [64].

(iv-III) Polarization control of IJJ THz sources

Controlling of the polarization is of especial importance in many applications of THz waves, for example in THz imaging, sensing, spectroscopy, high-speed and wireless telecommunication, etc [73-76]. The IJJ THz sources can be an excellent THz source for these purposes because (i) they have a unique ultra-wideband tunability and (ii) their emission intensity can be (internally and externally) thermally controlled [77-80].

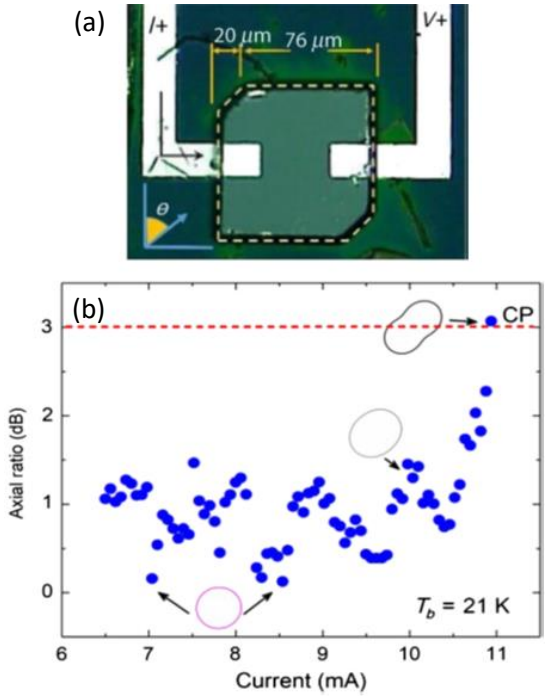

Fig. 7. (a) Optical microscopic images of the monolithic IJJ THz antenna that emits CP THz waves. (b) Axial ratio evolution (blue solid symbols) versus bias current of the IJJ monolithic THz antenna at T= 21 K [81].

IJJ THz devices with a rectangular cavity are known to emit linearly polarized light [26]. Asai *et al.* first theoretically demonstrated that circular polarized (CP) THz waves can be emitted from IJJ THz emitters that are locally heated by an external heat source, such as a laser [79]. This is because, in a square cavity, the laser would induce an inhomogeneity in the critical current density, that results in the excitation of the EM cavity TM (1,0) and TM (0,1) modes, whose polarizations are orthogonal to each other, so CP can be generated by a mixture of those two excited modes. They also showed that the CP can be dramatically controlled by the applied V.

Elarabi *et al.* later reported the first experimental demonstration of IJJ THz sources with the emission of CP THz waves, first from a monolithic THz source in which the ellipticity and evolution direction were tuned by the device geometry and voltage [81], and more recently from a cylindrical antenna [82]. Their highest degree of circular polarization (DOCP) from a monolithic IJJ THz emitter was 99.7%, which is considerably higher than that of QCLs [83-85].

Figure 7 (a), shows the microscopic image of one of the IJJ THz devices (with monolithic truncated-edge microstrip patch antennas) studied by Elarabi *et al.* for CP emission. Light emission with an axial ratio (AR), the ratio between the major and minor axes of the fitted polarization ellipse, less than 3 dB was attributed to a CP light. The CP THz wave emissions from these devices were obtained from the excitations of two transverse orthogonal modes along the major and minor diagonals [81,82]. The evolution of the polarization of the truncated-edge square antenna is plotted in Figs. 7 (b). The AR is shown as a function of bias current.

(v) Entirely liquid He-free IJJ THz sources

In a further development of IJJ THz devices, Hao *et al.* reported on a THz torch-like device operating at liquid nitrogen (LN_2) temperatures. The IJJ THz sources were surrounded by two gold layers, sandwiched between two MgO substrates and operated with a current I < 30 mA and a voltage V= 1.5 V [86]. The maximum emission power of such THz sources was 1.17 μW with a THz bandwidth of up to 100 GHz.

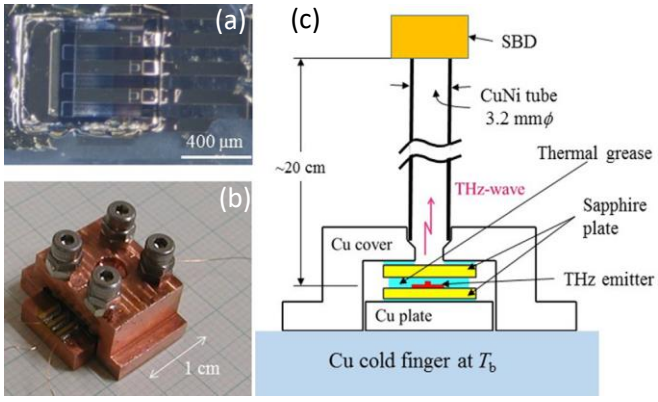

Fig. 8. (a) Optical image of three IJJ THz emitting devices on BSCCO single crystal, placed on sapphire substrate and operated in LN_2 temperatures. (b) Liquid He-free THz device module. (c) A cross-sectional sketch of the IJJ THz sources [87].

Subsequently, a liquid helium-free, compact source system operating at T= 77 K was developed by Minami *et al.* [87]. Their THz devices, see Fig. 8, were modified stand-alone rectangular emitters in a sandwich structure which experienced considerably reduced Joule heating. They used sapphire substrates and thin thermal grease surrounded by diamond nanocrystals to achieve good thermal conductivity of their THz devices. Intense THz radiation was observed in liquid N_2 temperatures with the excitation of the TM (1,0) cavity mode at f= 0.437 THz. This was the record maximum frequency attained at T= 77 K.

B. IJJ THz detectors

Novel superconductor-based THz detectors have enabled great advances in both civilian and military technologies. The THz range is also an important band for astronomical and cosmological observations. Absorption in the THz band is a useful diagnostic probe in medicine, biotechnology, biology, and agriculture, and for tracer-gas detection and for nondestructive evaluation. For all these applications, a highly sensitive and also integrated THz detector is required. IJJ devices of layered superconducting BSCCO have shown great potential as on-chip and integrated THz detectors. Here, we review the most recent IJJ based THz detectors that have been realized in integrated and on-chip THz circuitry.

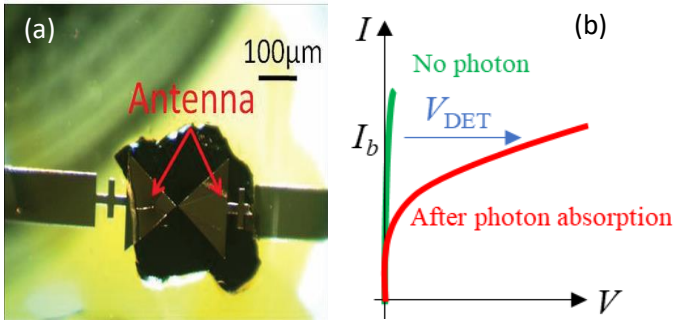

Fig. 9. (a) Optical image of the IJJ THz detector. Two antennas are shown by red arrows. (b) Principle of IJJ surface THz detector [88].

Figure 9 (a) presents the optical picture of the IJJ surface detector mesa with dimensions of 5 × 5 μm^2 integrated with a bow-tie antenna, as was reported by Irie *et al.* [88,89]. Thin IJJs were cut at the top of the BSCCO mesa, i.e., the so-called surface IJJs, with a surface (small) critical current I_c (in comparison to that of the rest of the stack) so such a device is very sensitive to an EM field. In an on-chip generator/detector configuration, the detector can be placed at a distance of 1 cm from the mesa generator and triggered by an independent bias circuit. The THz waves radiated from the generator mesa can be sensed by the modulation of V_{DET} (see Fig. 9 (b))- the I_c of the surface IJJ detector mesa is suppressed by absorbing the EM waves' power [88,90].

Most recently, Borodianskyi *et al.* demonstrated an integrated device on a single chip that operates in both THz generator and detector configurations [65]. The emitters and detectors were separated by a distance of ~25 μm as a separation chosen to minimize the undesired response to heating and non-equilibrium quasiparticle injection (see Fig. 10). The device contains nine mesa cavities. There are two generators and two detectors with considerably different shapes.

They used larger generators to attain higher overall THz power (which is proportional to the area). The BSCCO crystal used for THz chip fabrication was a strongly underdoped crystal with a T_c= 50 K, which results in a low critical current density J_c ~ 100 A/cm^2. Therefore, the mesas can be voltage biased up to ~10 V at a rather small bias current of I ~ 200 μA.

They used the smallest distant mesas as detectors because the smaller detectors harvest higher sensitivities (inversely proportional to the area). In the detector mesa, the few top IJJ layers were used as a switching current detector (with an independent control circuit) as they have a significantly smaller I_c owing to deterioration of the CuO layers on the BSCCO surface [65].

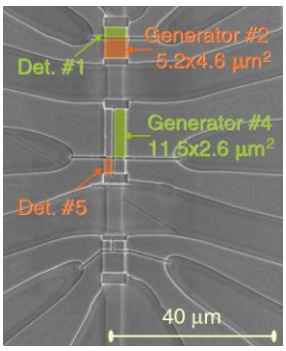

Fig. 10. Scanning electron microscopy image of an on-chip and integrated IJJ THz circuit comprising THz emitters, waveguides and detectors [65]. Two nearby mesas are used as detector mesas: mesa #5 with 1.2 × 3.3 μm^2 and mesa #1 with 5.2 × 2.3 μm^2 dimensions.

III. Applications Using IJJ Coherent THz Sources

We have shown that IJJ THz devices based on high-T_c BSCCO layered superconductors have the potential to be used in various applications and can be considered as the most promising THz devices, with the capability of operation in both generator/detector configurations, to bridge the gap between microwave and optics.

To prove this claim in this section we review several applications in which IJJ THz devices have been used, such as in THz transmission/reflection imaging, THz spectroscopy of liquids and gases, THz tomography, *etc*. We then review an effective technique for compactly-packaging these CW IJJ THz devices.

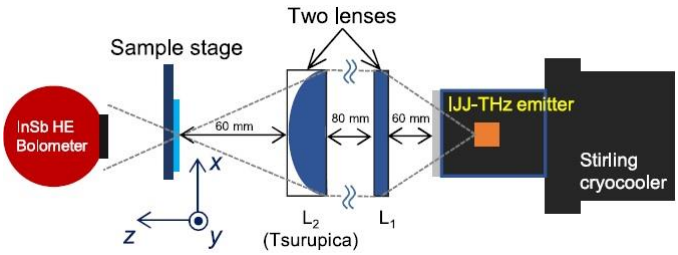

Fig. 11. Schematic diagram of an IJJ transmission THz imaging system [91].

A. THz Imaging

The ability to emit continuous and monochromatic THz waves with high spectral intensity, and high-frequency resolution, due to their intrinsic linewidth of as small as a few MHz, make IJJ THz devices very suitable for various THz imaging applications.

- *Transmission type imaging*

Using the amplitude modulation of THz radiation (monochromatic THz emission with f= 0.6 THz and Δ f= 0.5 GHz) from a rectangular IJJ THz emitter, fabricated by focused

ion beam (FIB) on the surface of BSCCO single crystal, the first experimental transmission THz imaging was reported in 2012 [40]. Later Nakade *et al* demonstrated a compact and user-friendly transmission THz imaging system (see Fig. 11) using a rectangular stand-alone IJJ THz emitter made by Ar milling as the THz source, a Stirling cryo-cooler engine, two THz lenses, an InSb hot-electron bolometer detector, a lock-in amplifier, two-dimensional scanning stage, an analog to digital converter, a function generator, and a temperature controller [91]. The system could be easily operated down to T= 40 K. They have also developed a home-built Michelson type of interferometer for the realization of phase-sensitive imaging systems.

To demonstrate the performance of the THz transmission imaging system, two samples, (i) an integrated circuit (IC) card [91] and (ii) a thin razor blade placed inside a brown paper envelope, were considered [40] (see Fig. 12). The scanning step of THz imaging for the IC card sample was 0.5 mm. As evidence of high-quality THz imaging, Fig. 12 (b) shows the region which is surrounded by a dotted box in Fig. 12 (a). The transmission THz image that was taken with scan steps of 0.2 mm clearly showed that inside the plastic body of the IC card, a comb-shaped structure exists. The 1.3 mm distance between each part of the comb was also clearly captured.

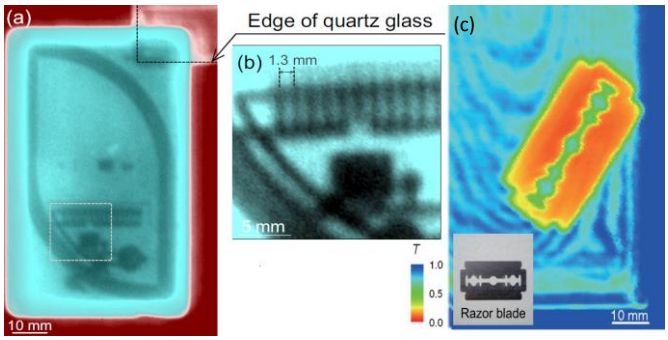

Fig. 12. (a) Transmission THz image of an IC card with scanning steps of 0.5 mm. (b) THz image scanned over the region surrounded by the dotted rectangle in (a) with scanning steps of 0.2 mm [91]. (c) THz image of a razor blade placed inside the brown paper envelope. The optical image of the object is also shown [40].

- *Reflection type imaging*

To demonstrate the additional capability of monochromatic radiation from IJJ THz devices, a reflection THz imaging system was also demonstrated by Kashiwagi *et al* [85]. The advantages of reflection THz imaging system is that in contrast to transmission THz imaging, here THz waves do not need to penetrate through the objects. With this technique and reflectivity measurements, the surface structures of the object under test and related information can be inferred [92].

As an example, we show how the IJJ-THz emitter was used in a security application. Figure 13 shows the photograph of a kitchen knife which was covered by up to five layers newspaper. The reflection THz imaging was taken using a conventional IJJ THz source of 60 × 400 × 1.6 μm^3 dimensions with monochromatic THz frequency f= 510 GHz [92]. In this system similar to the transmission THz imaging system, InSb was used as the THz detector. The device THz power recorded by the detector was approximately 34 μW- good enough for performing reflection THz imaging with a signal/noise ratio of around a hundred. A clean image of the bare knife not covered by the newspaper is shown in Fig. 13 (b). By increasing the number of wrapping sheets, the quality of the image reduces (see Fig. 13 (d-f)). This is due to the THz wave scattering and also THz beam decay at each newspaper layer. Image quality was lost for more than five layers of newspaper. These types of issues may be resolved if powerful IJJ THz sources of stand-alone or array devices are realized.

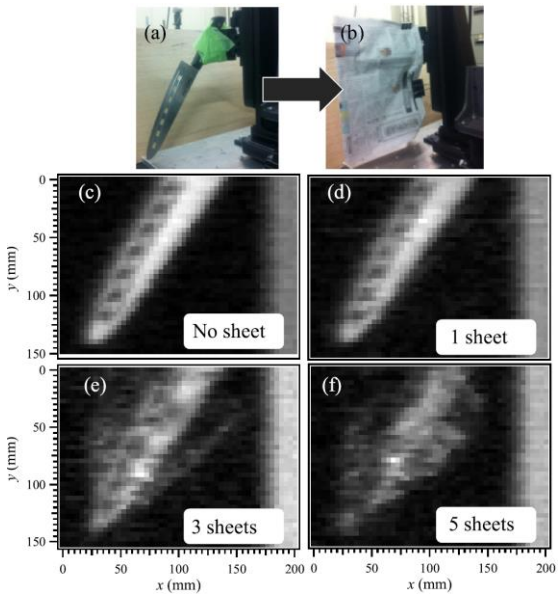

Fig. 13. Optical images of a kitchen knife under test (a) and the knife covered in a newspaper (b). THz reflection images of the kitchen knife, not covered (c), and covered by: one sheet layer (d), three sheet layers (e) and five sheet layers of newspaper [92].

B. THz spectroscopy of liquids and gases with IJJ THz sources

The EM waves, especially in the range of frequencies from MWs to IR, are strongly absorbed by liquids. Tsujimoto *et. al.* reported the first application of IJJ THz sources in the spectroscopy of liquids in 2012 [40]. A handmade (wedged-shaped) interferometer quartz cell was used, and distilled water and 99.5% pure ethanol were injected into it. The absorption coefficients of these liquids were then studied with 99.2% accuracy by scanning the wedge linearly from the thinner finish to the thicker finish [40].

Later, Nakade *et al.* demonstrated temperature-dependent measurements of the absorption coefficient of pure water with a resistivity of more than 1 MΩ.cm at 25 °C and compared their results with data reported in the literature from a THz-TDS system [91]. They found that their results on the absorption coefficient of water were very accurate. The signal-to-noise ratio in this frequency region was much higher than that of other techniques.

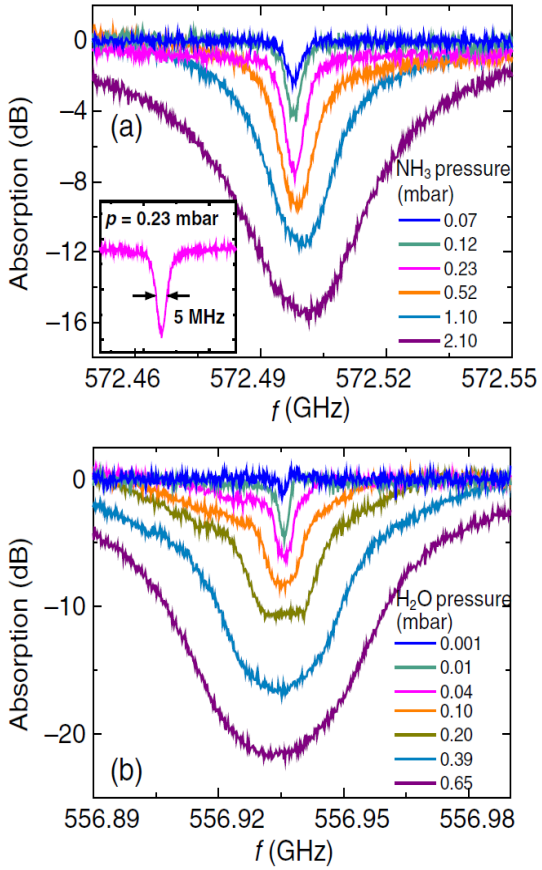

Fig. 14. THz spectroscopy using IJJ THz sources. (a) absorption lines of ammonia (mixed with water; 10% solution). (b) water vapor at different pressures. (Inset) Absorption line of ammonia vapor at P= 0.23 mbar, with an absorption linewidth of 5 MHz [93].

Further, in this direction, Sun *et al.* reported on spectrometric gas detection using IJJ THz sources [93]. They have employed both bolometric and heterodyne detection methods for the THz detection of absorption dips of water (H_2O) and ammonia (NH_3) vapor. The minimum detectable gas pressure they attained was around 0.001 mbar for H_2O and about 0.07 mbar for NH_3, with the smallest absorption linewidths in the range of 4 to 5 MHz in their systems.

Figure 14 (a) shows the THz absorption lines of diluted ammonia (NH_3) (mixed with water; 10% solution) and (b) water (H_2O) vapor at different pressures. In their experiment, an IJJ emitter and a superconducting integrated receiver (SIR) were used as the THz source and detector, respectively. Devices were operated at temperature T= 4.2 K. The absorption lines of NH_3 and H_2O were increased at large gas pressures. However, the linewidth reduced as pressure was decreased. They observed a clear absorption dip for NH_3 with an absorption linewidth of around 5 MHz (inset of Fig. 14) at P= 0.23 mbar (on the order of the concentration of trace gases) [93].

C. *THz tomography*

THz waves can enter various thin materials such as skin, paper, plastic, *etc*, therefore THz imaging systems offer the possibility of sensing objects (with high THz absorption coefficients) that are covered, hidden or latent. THz imaging systems with transmission or reflection configurations deliver information about the surface/bulk structures of materials and can be used for characterization of materials, layers inspection, *etc*. Furthermore, a THz computed tomography (THz-CT) imaging system can deliver cross-sectional insight into the material's interior structure [94].

During THz tomography measurements, to attain reliable and consistent computed tomography (CT) images, a stable and high-power beam of THz signal is required. Kashiwagi *et al.* developed a CT imaging system and used a monochromatic IJJ THz source, consisting of an 80 × 400 × 2.4 μm^3 rectangular superconducting cavity. It radiates THz waves at f= 0.44 THz, T = 40K, with a stable THz power of around 34 nW, adequate for *ac* voltage bias modulation measurements. They have demonstrated three different CT measurements of standing metallic rods, a dried plant (heart pea), and a plastic doll inside an eggshell [94].

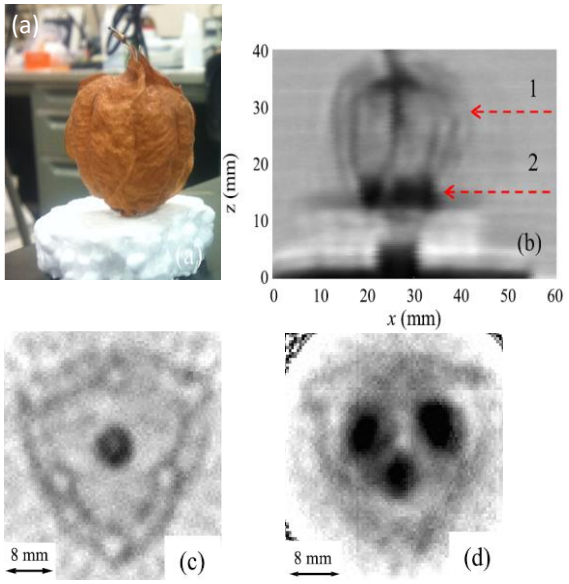

Fig. 15. Optical photograph of a dried heart pea. (b) Transmission THz image of the dried heart pea. Horizontal planar THz-CT images of regions showed by dashed red arrows 1 (c) and 2 (d) in Fig. 14, taken at fixed z values. The horizontal images for the THz CT image are taken at a scanning speed of 10 mm/s along x in measurement steps of 0.4 mm [94].

As an example, the THz-CT scan of a dried heart pea with three seeds inside will be reviewed here. Figure 15 (a) is the picture of a heart pea on the piece of styrofoam. Figure 15 (b) is the 2D transmission THz-image, which clearly shows the image of the heart pea bottom with three dark spots- that are

found to be heart pea's seeds (see Fig. 15 (a) for an exterior view). The vague perpendicular lines, from top to bottom, are three wall layers between the heart pea's ventricles.

Figures 15 (c) and (d) are the THz-CT images of the heart pea built by 36 transmission 2D THz images at the horizontal planes marked by the red dashed arrows 1 and 2 in Fig. 15 (b), respectively. It is interesting to see that Fig. 15 clearly demonstrates the CT THz characteristic structures of a heart pea with three ventricles, a balloon-like triangular capsule that is constrained together, and three ball-like seeds located in each ventricle. The demonstration of THz-CT of objects such as seeds inside a dried heart pea and a hidden doll inside the eggshell suggest that IJJ THz sources are strong enough to be widely used in transmission THz-CT imagining systems for different THz imaging purposes.

IV. Packaging

In making these devices portable and user-friendly for various applications, Tsujimoto *et al.* developed techniques for engineering of these devices and demonstrated a sub-centimeter sized THz source module [95]. They manufactured a portable and compact THz emitter device, which consists of an IJJ THz laser device, circuit bias electrodes, a collimating lens, and related apparatuses, all of which were wrapped into a single finger-sized assembly.

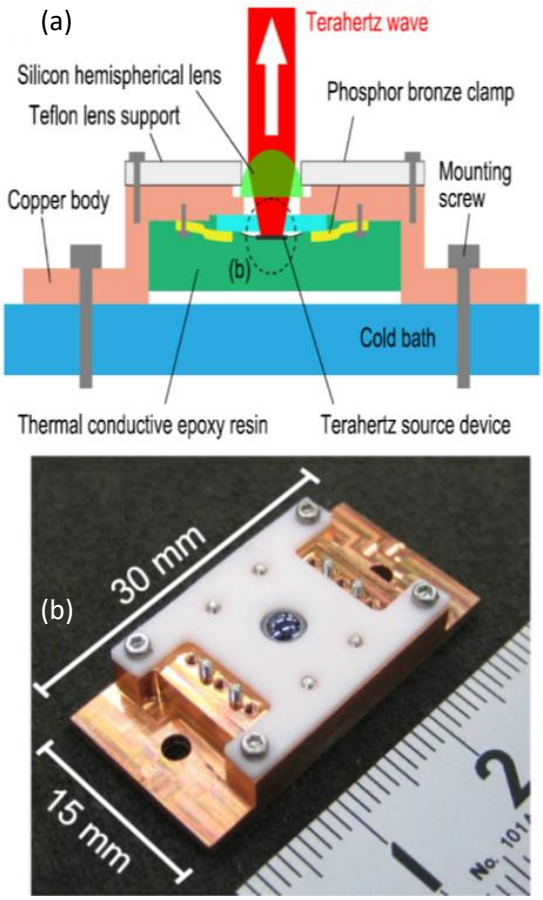

Fig. 16. (a) Cross-section sight of the IJJ THz source module. IJJ THz sources radiates CW THz signal to free space through silicon lens. (b) Photo of the assembled IJJ THz module [95]: a portable, compact and pocket THz laser.

They demonstrated that the device module is user-friendly and offers reproducible characteristics with a high-yield rate and low screening.

Figures 16 (a) and (b) show the cross-sectional schematic view and a picture of the packed THz source module, respectively. The module is compact, with $15 \times 30 \times 5.5$ mm^3 dimensions.

The effect of the packaging on the device's thermal properties was also quantitatively and qualitatively investigated by COMSOL modeling, and they found that to manage the overheating, the effective area at the contact surface has to be large. They also found that using sapphire with its high thermal conductivity may result in the homogeneous temperature spreading over the whole substrate.

The sub-centimeter (finger-tip) dimension IJJ THz source modules with high yield, efficient thermal conductivity, and both physical and chemical stabilities demonstrated in this study suggest its ease of operation as a portable THz source. The module only requires a current $I < 30$ mA and a voltage $V = 1.5$ V to operate, just like a quantum THz torch, paving the way for its practical usage and integration in various types of THz system and set up [81,86,95]. An example of a THz setup with an IJJ emitter as a circularly polarized THz light source is shown in Fig. 17 [81].

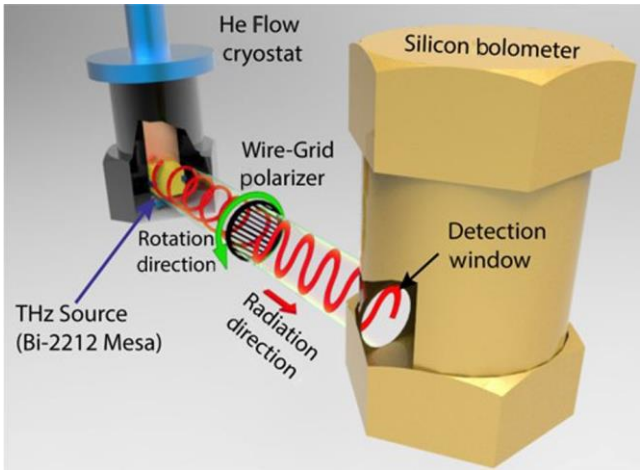

Fig. 17. An example of THz setup with an IJJ THz emitter as a source of circularly polarized light [81].

V. Future Plans and Perspective

Results presented in previous sections provide strong evidence that the broadly tunable IJJ-based THz devices can compete with existing solid-state THz sources, such as RTDs and QCLs, due to their large tunability- that covers entire THz gap- as well as the high degree of circular polarization of the emitted radiation. They can be applied to many practical applications. THz imaging technologies based on IJJ THz devices are enormously valuable for studying and characterizing objects that have diverse THz absorption coefficients. We showed that IJJ THz devices can be operated in both THz wave oscillator and detector configurations, paving the way for on-chip THz spectroscopy.

In fulfilling *THz on a chip* system for commercially viable IJJ THz technology (a single chip with integrated THz components such as IJJ sources and detectors, superconducting waveguides, receivers, etc) the synthesis of large-area epitaxial thin films of BSCCO is required. The recently developed method of liquid-phase epitaxial grown thick BSCCO film could be a promising candidate platform for this purpose [96]. THz devices based on such a 2D platform would benefit from low loss substrates that are highly thermally conductive, so thermal conductivity of the devices can be controlled. This technique may lead to stronger THz radiation and make possible the realization of low-loss superconducting THz components such as waveguides and couplers for the integration of IJJ THz modules.

Integration of superconducting BSCCO split-ring resonators (SRR), Fig. 18 (a), with IJJ THz emitters and detectors, can improve the THz devices' functionalities and allows control over device polarization, emission pattern directivity, and output power [97].

Compact arrays of thermally managed BSCCO microstrip antennas can also be realized. Two sketches of possible compact arrays are shown in Fig. 18. In Fig. 18 (b), a hexagonal close-packed two-dimensional array of seven thermally managed BSCCO disks, each cut into six equivalent pie-shaped wedges, is shown [24,26,48]. In Fig. 18 (c), each of the seven six-fold slitted disks, is further subject to a circular slit, producing 42 pie-shaped antennas and 42 slitted annular antennas. The non-degenerate wave functions for such slitted annular antennas with Neumann boundary conditions are easily obtained analytically. Moreover, such devices are relatively easy to manufacture [35,55].

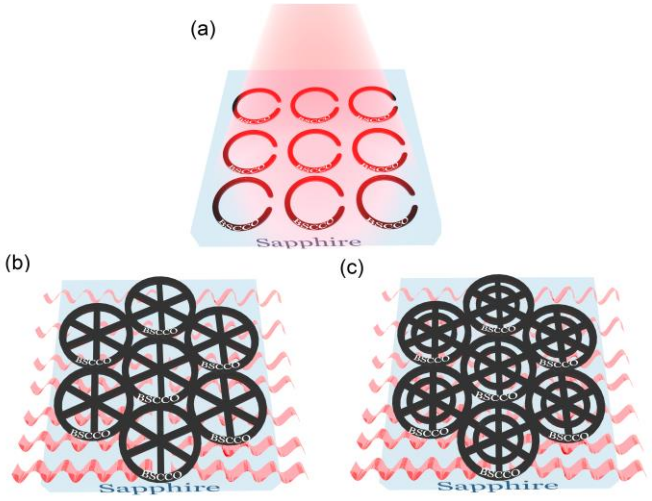

Fig. 18: (a) Schematic diagram of array of BSCCO SRR on the sapphire substrate [97]. (b) and (c) Sketches of possible hexagonal close-packed arrays of equivalent BSCCO microstrip antennas with non-degenerate cavity mode frequencies. (b) Array of 42 pie-shaped wedge antennas. (c) Array of 42 pie-shaped wedge antennas and 42 six-fold slitted annular antennas.

ACKNOWLEDGMENT

K. Delfanazari acknowledges support from the JST-CREST (for Research Assistantship), the Japanese Ministry of Education, Culture, Sports, Science, and Technology (Monbu-kagaku-shō for scholarship), the EPSRC UK (for grant No. EP/S019324/1), and would like to thank Drs. T. Kashiwagi, M. Tsujimoto, I. Kakeya, H. Wang, T. Yamamoto, H. Asai, H. Minami, T. Hattori, and H. Beere for many helpful discussions.

REFERENCES

[1] Y.-S. Lee, in *Principles of Terahertz Science and Technology*, Berlin, Germany, Springer, 2008.
[2] M. Tonouchi, "Cutting-edge terahertz technology," *Nat. Photon.*, vol. 1, pp. 97–105, 2007.
[3] S S Dhillon et al, The 2017 terahertz science and technology roadmap, *J. Phys. D: Appl. Phys*. 50 pp. 043001, 2017.
[4] M. A. Richards, W. A. Holm, J. Scheer, in *Principles of Modern Radar: Basic Principles*, SciTech Pub., pp. 360. 2010.
[5] H. R. Johnson, "Backward-wave oscillators," *Proceedings of the IRE*, vol. 43(6), pp. 684-697, 1955.
[6] Z. Huang, K. J. Kim, "Review of x-ray free-electron laser theory," *Phys. Rev. Accel. Beams.*, vol. 10 (3), PP. 034801, 2007.
[7] E. M. Rowe and F. E. Mills, "Tantalus I: a dedicated storage ring synchrotron radiation source," *Particle Accelerators*, vol. 4, pp. 211-227, l973.
[8] F. Hindle, A. Cuisset, R. Bocquet, G. Mouret, "Continuous-wave terahertz by photomixing: applications to gas phase pollutant detection and quantification," *CR Phys*., vol. 9, pp. 262-275, 2008.
[9] P. R. Smith, D. H. Auston, and M. C. Nuss, "Subpicosecond photoconducting dipole antennas," *IEEE J. Quantum Electron*. vol. 24, pp. 255–260 (1988).
[10] M. B. Johnston, D. M. Whittaker, A. Corchia, A. G. Davies, E. H. Linfield, "Simulation of terahertz generation at semiconductor surfaces," *Phys. Rev. B.* vol. 65, pp. 5401J, 2002.
[11] H. Ito, F. Nakajima, T. Furuta, & T. Ishibashi, "Continuous THz-wave generation using antenna-integrated uni-traveling-carrier photodiodes," *Semicond. Sci. Technol.* 20, S191–S198 (2005).
[12] T. H. Lee, "Planar microwave engineering: a practical guide to theory, measurement, and circuits," Cambridge University Press, pp. 296, 2004. ISBN 0521835267
[13] S. Marsh, "Practical MMIC Design,", Artech House, Kindle edition, 2006.
[14] M. Theuer, G. Torosyan, C. Rau R. Beiganga, K. Maki, C. Otani, and K. Kawase, "Efficient generation of Cherenkov-type terahertz radiation from a lithium niobate crystal with a silicon prism output coupler," *Appl. Phys. Lett.*, vol. 88, pp.071122, 2006.
[15] M. Asada, S. Suzuki and N. Kishimoto, Resonant Tunneling Diodes for Sub-Terahertz and Terahertz Oscillators, *Jpn. J. Appl. Phys*. 47 pp. 4375, 2008.
[16] K. Kasagi, S. Suzuki, and M. Asada, "Large-scale array of resonant-tunneling-diode terahertz oscillators for high output power at 1 THz," *J. Appl. Phys.* vol. 125, pp. 151601, 2019.
[17] F. Jerome, F. Capasso, D. L. Sivco, C. Sirtori, A. L. Hutchinson, A. Y. Cho, "Quantum Cascade Laser," *Science*, vol. 264 Art.no. 5158, pp. 553–556, 1994.
[18] G. Scalari, L. Ajili, J. Faist, H. Beere, E. Linfield, D. Ritchie, G. Davies, "Far-infrared (λ = 87 μm) bound-to-continuum quantum-cascade lasers operating up to 90 K," *Appl. Phys. Lett.*, vol. 82, pp. 3165, 2003.
[19] S. Barbieri, J. Alton, H. E. Beere, J. Fowler, E. H. Linfield and D. A. Ritchie, "THz quantum cascade lasers operating up to 70K in a continuous wave," *Appl. Phys. Lett.*, vol. 85, pp. 1674–1676, 2004.
[20] Q. Y. Lu, N. Bandyopadhyay, S. Slivken, Y. Bai, and M. Razeghi, "Continuous operation of a monolithic semiconductor terahertz source at room temperature," *Appl. Phys. Lett.*, vol. 104, pp. 221105, 2014.
[21] M. A. Belkin, F. Capasso, F. Xie, A. Belyanin, M. Fischer, A. Wittmann, and J. Faist, "Room temperature terahertz

quantum cascade laser source based on intracavity difference-frequency generation," *Appl. Phys. Lett.*, vol. 92, pp. 2011201, 2008.

[22] B. D. Josephson, "Possible new effects in superconductive tunneling," *Phys. Rev. Lett*., vol. 1, pp. 251–253 (1962).

[23] H. Maeda, Y. Tanaka, M. Fukutumi, T. Asano, "A new high-T_c oxide superconductor without a rare earth element," *Jpn. J. Appl. Phys.*, vol. 27 (2), pp. l209–l210 (1988).

[24] M. A. Subramanian *et al.*, "A new high-temperature superconductor: $Bi_2Sr_{3-x}Ca_xCu_2O_{8+y}$," *Science* vol. 239 pp. 1015–1017, 1988, Art. no. 4843.

[25] R. Kleiner, F. Steinmeyer, G. Kunkel, and P. Müller, "Intrinsic Josephson effects in $Bi_2Sr_2CaCu_2O_8$ single crystals," *Phys. Rev. Lett.*, vol. 68, 1992, Art. no. 2394

[26] L. Ozyuzer, A.E. Koshelev, C. Kurter, N. Gopalsami, Q. Li, M. Tachiki, K. Kadowaki, T. Yamamoto, H. Minami, H. Yamaguchi, T. Tachiki, K.E. Gray, W.-K. Kwok, U. Welp, "Emission of coherent THz radiation from superconductors," *Science*, vol. 318, 2007, Art. no. 1149802.

[27] K. Kadowaki, H. Yamaguchi, K. Kawamata, T. Yamamoto, H. Minami, I. Kakeya, U. Welp, L. Ozyuzer, A. Koshelev, C. Kurter, K. E. Gray, W.-K. Kwok, "Direct observation of terahertz electromagnetic waves emitted from intrinsic Josephson junctions in single crystalline $Bi_2Sr_2CaCu_2O_{8+\delta}$," *Physica C*, vol. 468, pp. 634, 2008.

[28] R. Kleiner, and P. Müller, "Intrinsic Josephson Effects in High-T_c Superconductors," *Phys. Rev. B*, vol. 49, no. 2, 1994, Art. no. 1327-1341

[29] I. E. Batov, X. Y. Jin, S. V. Shitov, Y. Koval, P. Müller, and A. V. Ustinov, "Detection of 0.5 THz radiation from intrinsic $Bi_2Sr_2CaCu_2O_8$ Josephson junctions," *Appl. Phys. Lett*. vol. 88, 2006, Art. no. 262504.

[30] K. Kadowaki, M. Tsujimoto, K. Delfanazari, T. Kitamura, M. Sawamura, H. Asai, T. Yamamoto, K. Ishida, C. Watanabe, S. Sekimoto, K. Nakade, T. Yasui, K. Asanuma, T. Kashiwagi, H. Minami, M. Tachiki, T. Hattori, R. A. Klemm, "Quantum terahertz electronics (QTE) using coherent radiation from high temperature superconducting $Bi_2Sr_2CaCu_2O_{8+d}$ intrinsic Josephson junctions," *Physica C*, vol. 491, pp. 2-6, 2013.

[31] K. Delfanazari, H. Asai, M. Tsujimoto, T. Kashiwagi, T. Kitamura, K. Ishida, C. Watanabe, S. Sekimoto, T. Yamamoto, H. Minami, M. Tachiki, R.A. Klemm, T. Hattori, and K. Kadowaki, "Terahertz oscillating devices based upon the intrinsic Josephson junctions in a high temperature superconductor," *J. Infrared, Millimeter, Terahertz Waves*, vol. 35, no. 1, pp. 131–146, 2014.

[32] U. Welp, K. Kadowaki, and R. Kleiner, "Superconducting emitters of THz radiation," *Nat. Photonics*, vol. 7, pp. 702, 2013.

[33] K. Delfanazari, H. Asai, M. Tsujimoto, T. Kashiwagi, T. Kitamura, T. Yamamoto, M. Sawamura, K. Ishida, C. Watanabe, S. Sekimoto, H. Minami, M. Tachiki, R.A. Klemm, T. Hattori, and K. Kadowaki, "Tunable terahertz emission from the intrinsic Josephson junctions in acute isosceles triangular $Bi_2Sr_2CaCu_2O_{8+\delta}$ mesas," *Opt. Express*, vol. 21, no. 2, pp. 2171–2184, 2013.

[34] K. Delfanazari, H. Asai, M. Tsujimoto, T. Kashiwagi, T. Kitamura, T. Yamamoto, M. Sawamura, K. Ishida, M. Tachiki, R.A. Klemm, T. Hattori, and K. Kadowaki, "Study of coherent and continuous terahertz wave emission in equilateral triangular mesas of superconducting $Bi_2Sr_2CaCu_2O_{8+\delta}$ intrinsic Josephson junctions," *Phys. C Supercond. its Appl.*, vol. 491, no. August, pp. 16–19, 2013.

[35] M. Tsujimoto, T. Yamamoto, K. Delfanazari, R. Nakayama, T. Kitamura, M. Sawamura, T. Kashiwagi, H. Minami, M. Tachiki, K. Kadowaki, and R.A. Klemm, "Broadly tunable subterahertz emission from Internal Branches of the current-Voltage characteristics of superconducting $Bi_2Sr_2CaCu_2O_{8+\delta}$ single crystals," *Phys. Rev. Lett.*, vol. 108, no. 10, pp. 1–5, 2012.

[36] T. Kashiwagi, M. Tsujimoto, T. Yamamoto, H. Minami, K. Yamaki, K. Delfanazari, K. Deguchi, N. Orita, T. Koike, R. Nakayama, T. Kitamura, M. Sawamura, S. Hagino, K. Ishida, K. Ivanovic, H. Asai, M. Tachiki, R.A. Klemm, and K. Kadowaki ,"High temperature superconductor terahertz emitters: Fundamental physics and its applications," *Jpn. J. Appl. Phys.*, vol. 51, no. 1, pp. 1–14, 2012.

[37] R.A. Klemm, K. Delfanazari, M. Tsujimoto, T. Kashiwagi, T. Kitamura, T. Yamamoto, M. Sawamura, K. Ishida, T. Hattori, and K. Kadowaki, "Modeling the electromagnetic cavity mode contributions to the THz emission from triangular $Bi_2Sr_2CaCu_2O_{8+\delta}$ mesas," *Phys. C Supercond. its Appl.*, vol. 491, pp. 30–34, 2013.

[38] K. Delfanazari, H. Asai, M. Tsujimoto, T. Kashiwagi, T. Kitamura, T. Yamamoto, W. Wilson, R.A. Klemm, T. Hattori, and K. Kadowaki, "Effect of Bias Electrode Position on Terahertz Radiation from Pentagonal Mesas of Superconducting $Bi_2Sr_2CaCu_2O_{8+\delta}$," *IEEE Trans. terahertz Sci. Technol.*, vol. 5, no. 3, pp. 505–511, 2015.

[39] R.A. Klemm, A.E. Davis, Q.X. Wang, T. Yamamoto, D.P. Cerkoney, C. Reid, M.L. Koopman, H. Minami, T. Kashiwagi, J.R. Rain, C.M. Doty, M.A. Sedlack, M.A. Morales, C. Watanabe, M. Tsujimoto, K. Delfanazari, and K. Kadowaki, "Terahertz emission from the intrinsic Josephson junctions of high-symmetry thermally-managed $Bi_2Sr_2CaCu_2O_{8+\delta}$ microstrip antennas," *IOP Conf. Ser. Mater. Sci. Eng.*, vol. 279, no. 1, p. 012017, Dec. 2017.

[40] M. Tsujimoto, H. Minami, K. Delfanazari, M. Sawamura, R. Nakayama, T. Kitamura, T. Yamamoto, T. Kashiwagi, T. Hattori, and K. Kadowaki, "Terahertz imaging system using high- T_c superconducting oscillation devices," *J. Appl. Phys.*, vol. 111, no. 12, p. 123111, Jun. 2012.

[41] K. Kadowaki, M. Tsujimoto, K. Delfanazari, T. Kitamura, M. Sawamura, H. Asai, T. Yamamoto, K. Ishida, C. Watanabe, S. Sekimoto, K. Nakade, T. Yasui, K. Asanuma, T. Kashiwagi, H. Minami, M. Tachiki, T. Hattori, and R.A. Klemm, "Quantum terahertz electronics (QTE) using coherent radiation from high temperature superconducting $Bi_2Sr_2CaCu_2O_{8+\delta}$ intrinsic Josephson junctions," *Phys. C Supercond.*, vol. 491, pp. 2–6, Aug. 2013.

[42] T. Kitamura, T. Kashiwagi, M. Tsujimoto, K. Delfanazari, M. Sawamura, K. Ishida, S. Sekimoto, C. Watanabe, T. Yamamoto, H. Minami, M. Tachiki, and K. Kadowaki, "Effects of magnetic fields on the coherent THz emission from mesas of single crystal $Bi_2Sr_2CaCu_2O_{8+\delta}$," *Phys. C Supercond. its Appl.*, vol. 494, pp. 117–120, 2013.

[43] D.P. Cerkoney, C. Reid, C.M. Doty, A. Gramajo, T.D. Campbell, M.A. Morales, K. Delfanazari, M. Tsujimoto, T. Kashiwagi, T. Yamamoto, C. Watanabe, H. Minami, K. Kadowaki, and R.A. Klemm, "Cavity mode enhancement of terahertz emission from equilateral triangular microstrip antennas of the high-Tc superconductor $Bi_2Sr_2CaCu_2O_{8+\delta}$," *J. Phys. Condens. Matter*, vol. 29, no. 1, p. 15601, 2017.

[44] T. Kashiwagi, T. Yamamoto, H. Minami, M. Tsujimoto, R. Yoshizaki, K. Delfanazari, T. Kitamura, C. Watanabe, K. Nakade, T. Yasui, K. Asanuma, Y. Saiwai, Y. Shibano, T. Enomoto, H. Kubo, K. Sakamoto, T. Katsuragawa, B. Marković, J. Mirković, R.A. Klemm, and K. Kadowaki, "Efficient Fabrication of Intrinsic-Josephson-Junction Terahertz Oscillators with Greatly Reduced Self-Heating Effects," *Phys. Rev. Appl.*, vol. 4, no. 5, p. 054018, 2015.

[45] T. Kashiwagi, T. Yamamoto, T. Kitamura, K. Asanuma, C. Watanabe, K. Nakade, T. Yasui, Y. Saiwai, Y. Shibano, H. Kubo, K. Sakamoto, T. Katsuragawa, M. Tsujimoto, K. Delfanazari, R. Yoshizaki, H. Minami, R.A. Klemm, and K. Kadowaki, "Generation of electromagnetic waves from 0.3 to 1.6 terahertz with a high- T c superconducting $Bi_2Sr_2CaCu_2O_{8+\delta}$ intrinsic Josephson junction emitter," *Appl. Phys. Lett.*, vol. 106, no. 9, pp. 0–5, 2015.

[46] K. Kadowaki, T. Kashiwagi, H. Asai, M. Tsujimoto, M. Tachiki, K. Delfanazari, and R.A. Klemm, "Terahertz Wave Emission from Intrinsic Josephson Junctions in $Bi_2Sr_2CaCu_2O_{8+\delta}$," *J. Phys. Conf. Ser.*, vol. 400, p. 022041, Dec. 2012.

[47] K. Delfanazari, M. Tsujimoto, T. Kashiwagi, T. Yamamoto, R. Nakayama, S. Hagino, T. Kitamura, M. Sawamura, T. Hattori, H. Minami, and K. Kadowaki, "THz emission from a triangular mesa structure of Bi-2212 intrinsic Josephson junctions," *J. Phys. Conf. Ser.*, vol. 400, p. 022014, 2012.

[48] M. Tsujimoto, T. Yamamoto, K. Delfanazari, R. Nakayama, N. Orita, T. Koike, K. Deguchi, T. Kashiwagi, H. Minami, and K. Kadowaki, "THz-wave emission from inner I-V branches of intrinsic Josephson junctions in $Bi_2Sr_2CaCu_2O_{8+\delta}$," *J. Phys. Conf. Ser.*, vol. 400, p. 022127, Dec. 2012.

[49] Kashiwagi, K. Deguchi, M. Tsujimoto, T. Koike, N. Orita, K. Delfanazari, R. Nakayama, T. Kitamura, S. Hagino, M. Sawamura, T. Yamamoto, H. Minami, and K. Kadowaki, "Excitation mode characteristics in Bi2212 rectangular mesa structures," *J. Phys. Conf. Ser.*, vol. 400, p. 022050, Dec. 2012.

[50] K. Delfanazari, H. Asai, M. Tsujimoto, T. Kashiwagi, T. Kitamura, T. Yamamoto, W. Wilson, R.A. Klemm, T. Hattori, and K. Kadowaki, "The influence of electrode position on the current-voltage characteristics and terahertz radiation in a high-T_c superconducting device," in *40th International Conference on Infrared, Millimeter, and Terahertz waves (IRMMW-THz)*, 2015. Electronic ISBN No. 978-1-4799-8272-1.

[51] K. Kadowaki, M. Tsujimoto, K. Delfanazari, T. Kitamura, M. Sawamura, T. Kashiwagi, H. Minami, M. Tachiki, and R.A. Klemm, "High power THz radiation from high-T_c superconducting intrinsic Josephson devices," in *37th International Conference on Infrared, Millimeter, and Terahertz Waves*, 2012. Print ISBN No. 978-1-4673-1598-2.

[52] K. Delfanazari, H. Asai, M. Tsujimoto, T. Kashiwagi, T. Kitamura, M. Sawamura, K. Ishida, T. Yamamoto, T. Hattori, R.A. Klemm, and K. Kadowaki, "Experimental and theoretical studies of mesas of several geometries for terahertz wave radiation from the intrinsic Josephson junctions in superconducting $Bi_2Sr_2CaCu_2O_{8+\delta}$," in *37th International Conference on Infrared, Millimeter, and Terahertz Waves*, 2012. Print ISBN No. 978-1-4673-1598-2.

[53] L. Ozyuzer, Y. Simsek, H. Koseoglu, F. Turkoglu, C. Kurter, U. Welp, A.E. Koshelev, K.E. Gray, W.K. Kwok, T. Yamamoto and K. Kadowaki, "Terahertz wave emission from intrinsic Josephson junctions in high-T_c superconductors," *Supercond. Sci. Technol.*, vol. 22, no. 11, 2009.

[54] I. Kakeya and H. Wang, "Terahertz-wave emission from Bi2212 intrinsic Josephson junctions: a review on recent progress," *Supercond. Sci. Technol*., vol. 29, pp. 073001, 2016.

[55] K. Delfanazari, R A Klemm, M. Tsujimoto, D. P Cerkoney, T. Yamamoto, T. Kashiwagi, K. Kadowaki, "Cavity modes in broadly tunable superconducting coherent terahertz sources ", *J. Phys: Conf. Seri*, vol. 1182, pp. 012011, 2019.

[56] N. Orita, H. Minami, T. Koike, T. Yamamoto and K. Kadowaki, Synchronized operation of two serially connected Bi2212 THz emitters *Physica C*, vol. 470, pp. S786, 2010.

[57] K. Kadowaki, M. Tsujimoto, K. Yamaki, T. Yamamoto, T. Kashiwagi, H. Minami, M. Tachiki and R. A. Klemm, "Evidence for a dual-source mechanism of THz radiation from rectangular mesas of single crystalline $Bi_2Sr_2CaCu_2O_{8+\delta}$ intrinsic Josephson junctions," *J. Phys. Soc. Jpn.* vol. 79, no. 2, pp. 023703, 2010.

[58] H. Asai, M. Tachiki and K. Kadowaki, "Numerical simulation of THz emission from two mesa structured intrinsic Josephson junctions," *J. Phys.: Conf. Ser*. vol. 400, pp. 022002, 2012.

[59] R. Klemm and K. Kadowaki, "Output from a Josephson stimulated terahertz amplified radiation emitter," *J. Phys.: Condens. Matter*, vol. 22, pp. 375701, 2010.

[60] R. Klemm and K. Kadowaki, "Angular dependence of the radiation power of a Josephson STAR-emitter," *J. Supercond. Novel Magn.* vol. 23, pp. 613, 2010.

[61] R. Klemm, E. LaBerge, D. Morley, T. Kashiwagi, M. Tsujimoto, K. Kadowaki, "Cavity mode waves during terahertz radiation from rectangular $Bi_2Sr_2CaCu_2O_{8+\delta}$ mesas," *J. Phys.: Condens. Matter*, vol. 23, pp. 025701, 2011.

[62] H. Asai, M. Tachiki and K. Kadowaki, "Three-dimensional numerical analysis of terahertz radiation emitted from intrinsic Josephson junctions with hot spots," *Phys. Rev. B*, vol. 85, pp. 064521, 2012.

[63] H. Asai, M. Tachiki and K. Kadowaki, "Proposal of terahertz patch antenna fed by intrinsic Josephson junctions," *Appl. Phys. Lett.*, vol. 101, pp. 112602, 2012.

[64] T. Kashiwagi, K. Sakamoto, H. Kubo, Y. Shibano, T. Enomoto, T. Kitamura, K. Asanuma, T. Yasui, C. Watanabe, K. Nakade, Y. Saiwai, T. Katsuragawa, M. Tsujimoto, R. Yoshizaki, T. Yamamoto, H. Minami, R. A. Klemm, K. Kadowaki, "A high-T_c intrinsic Josephson junction emitter tunable from 0.5 to 2.4 terahertz," *Appl. Phys. Lett.*, vol. 107, pp. 082601 (2015)

[65] E. Borodianskyi and V. Krasnov, "Josephson emission with frequency span 1–11 THz from small $Bi_2Sr_2CaCu_2O_{8+\delta}$ mesa structures," *Nat. Communications*, vol. 8, pp. 1742, 2017.

[66] T. M. Benseman, K. E. Gray, A. E. Koshelev, W.-K. Kwok, U. Welp, H. Minami, K. Kadowaki, and T. Yamamoto, "Powerful terahertz emission from $Bi_2Sr_2CaCu_2O_{8+\delta}$ mesa arrays," *Appl. Phys. Lett*. vol. 103, pp. 022602 (2013).

[67] T. Kitamura *et al* Broadly tunable, high-power terahertz radiation up to 73 K from a stand-alone $Bi_2Sr_2CaCu_2O_{8+\delta}$ mesa," *Appl. Phys. Lett.* vol. 105, pp. 202603, 2013.

[68] S. Sekimoto, C. Watanabe, H. Minami, T. Yamamoto, T. Kashiwagi, R. A. Klemm, and K. Kadowaki, "Continuous 30 μW terahertz source by a high-T_c superconductor mesa structure," *Appl. Phys. Lett.*, vol. 103, pp. 182601, 2013.

[69] X. Hu and S. Lin, "Cavity phenomena in mesas of cuprate highsuperconductors under voltage bias," *Phys. Rev. B*, vol. 80, 2009, Art ID 064519.

[70] A. E. Koshelev, "Resonant electromagnetic emission from intrinsic Josephson junction stacks with laterally modulated Josephson critical current," *Phys. Rev. B*, vol. 78, 2008, Art ID 174509.

[71] S. Savel'ev, V. A. Yampol'skii, A. L. Rakhmanov, and F. Nori, "Terahertz Josephson plasma waves in layered superconductors: spectrum, generation, nonlinear and quantum phenomena," *Rev. Prog. Phys*., vol. 73, 2010, Art ID 026501.

[72] Y. M. Shukrinov, I. R. Rahmonov, A. Plecenik , P. Seidel, E. Il'ichev and W. Nawrocki, Phase dynamics of two parallel stacks of coupled Josephson junctions, *Supercond. Sci. Technol.*, vol. 27, pp. 124007, 2014.

[73] S. A. Baig, J. L. Boland, D. A. Damry, H. Hoe Tan, C. Jagadish, H. J. Joyce, and M. B. Johnston, "An ultrafast switchable terahertz polarization modulator based on III–V semiconductor nanowires," *Nano Lett*., vol. 17, pp 2603–2610, 2017.

[74] S. J Kindness, N. W. Almond, W. Michailow, B. Wei, L. Jakob, K. Delfanazari, P. Braeuninger-Weimer, S. Hofmann, H. E Beere, D. A Ritchie, R. Degl'Innocenti, Graphene integrated metamaterial device for all electrical polarization control of terahertz quantum cascade lasers, *ACS Photonics*, 66 pp. 1547-1555, 2019.

[75] M. Jia, Z. Wang, H. Li, X. Wang, W. Luo, S. Sun, Y. Zhang, Q. He & L. Zhou, Efficient manipulations of circularly polarized terahertz waves with transmissive metasurfaces, *Light: Science & Applications*, vol. 8, Art. no: 16, 2019.

[76] X.-C. Zhang and J. Xu, in *Introduction to THz wave Photonics*, Berlin, Germany, Springer, 2009.

[77] H. B. Wang, S. Gu´enon, J. Yuan, A. Iishi, S. Arisawa, T. Hatano, T. Yamashita, D. Koelle, and R. Kleiner, "Hot spots and waves in $Bi_2Sr_2CaCu_2O_{8+\delta}$ intrinsic Josephson junction," *Phys. Rev. Lett.*, vol. 102, pp. 0017006, 2009.

[78] M. Tsujimoto, H. Kambara, Y. Maeda, Y. Yoshioka, Y. Nakagawa, and I. Kakeya, "Dynamic Control of Temperature Distributions in Stacks of Intrinsic Josephson Junctions in $Bi_2Sr_2CaCu_2O_{8+\delta}$," *Phys. Rev. Applied*, vol. 2, pp. 044016, 2014.

[79] H. Asai and S. Kawabata, "Control of circularly polarized THz wave from intrinsic Josephson junctions by local heating," *Appl. Phys. Lett.* vol. 110, pp. 132601, 2017.

[80] X. J. Zhou, J. Yuan, H. Wu, Z. S. Gao, M. Ji, D. Y. An, Y. Huang, F. Rudau, R. Wieland, B. Gross, N. Kinev, J. Li, A. Ishii, T. Hatano, V. P. Koshelets, D. Koelle, R. Kleiner, H. B. Wang, and P. H. Wu, "Tuning the Terahertz Emission

Power of an Intrinsic Josephson-Junction Stack with a Focused Laser Beam," *Phys. Rev. Applied*, vol. 3, pp. 044012 2015.
[81] A. Elarabi, Y. Yoshioka, M. Tsujimoto, and I. Kakeya, "Monolithic superconducting emitter of tunable circularly polarized terahertz radiation," *Phys. Rev. Appl.* vol. 8, pp. 064034, 2017.
[82] A. Elarabi, Y. Yoshioka, M. Tsujimoto, and I. Kakeya, "Circularly polarized terahertz radiation monolithically generated by cylindrical mesas of intrinsic Josephson junctions," *Appl. Phys. Lett.* vol. 113, pp. 052601, 2018.
[83] L. Xu, D. Chen, C. A. Curwen, M. Memarian, J. L. Reno, T. Itoh, and B. S. Williams, "Metasurface quantum-cascade laser with electrically switchable polarization," *Optica* vol. 4, pp. 468, 2017.
[84] P. Rauter, J. Lin, P. Genevet, S. P. Khanna, M. Lachab, A. Giles Davies, E. H. Linfield, and F. Capasso, "Electrically pumped semiconductor laser with monolithic control of circular polarization," *Proc. Natl. Acad. Sci. U.S.A.*, vol. 111, pp. E5623, 2014.
[85] G. Liang, Y. Zeng, X. Hu, H. Yu, H. Liang, Y. Zhang, L. Li, A. G. Davies, E. H. Linfield, and Q. J. Wang, Monolithic semiconductor lasers with dynamically tunable linear-tocircular polarization, *ACS Photonics*, vol.4, pp. 517, 2017.
[86] L. Y. Hao, M. Ji, J. Yuan, D. Y. An, M. Y. Li, X. J. Zhou, Y. Huang, H. C. Sun, Q. Zhu, F. Rudau, R. Wieland, N. Kinev, J. Li, W.W. Xu, B. B. Jin, J. Chen, T. Hatano, V. P. Koshelets, D. Koelle, R. Kleiner, H. B.Wang, and P. H.Wu, "Compact Superconducting Terahertz Source Operating in Liquid Nitrogen," *Phys. Rev. Applied*, vol. 3, pp. 024006, 2015.
[87] H. Minami, C. Watanabe, T. Kashiwagi, T. Yamamoto, K. Kadowaki and R A Klemm, "0.43 THz emission from high-Tc superconducting emitters optimized at 77 K," *J. Phys.: Condens. Matter*, vol. 28, pp. 025701, 2016.
[88] D. Oikawa, A. Irie , K. Yamaki , G. Oya, "Terahertz electromagnetic radiation from $Bi_2Sr_2CaCu_2O_{8+\delta}$ intrinsic Josephson junction stack," *Physics Procedia* vol. 27, pp. 312 –315, 2012.
[89] A. Irie, S. Heim, S. Schromm, M. Moßle, T. Nachtrab, M. Godo, R. Kleiner, P. Muller, G. Oya, "Critical currents of small $Bi_2Sr_2CaCu_2O_{8+\delta}$ intrinsic Josephson junction stacks in external magnetic fields," *Phys. Rev. B*, vol. 62, pp. 6681, 2000.
[90] A. Irie , D. Oikawa, G. Oya, "Generation and detection of THz radiation using intrinsic Josephson junctions," *Physics Procedia*, vol. 36, pp. 199–204, 2012.
[91] K. Nakade, T. Kashiwagi, Y. Saiwai, H. Minami, T. Yamamoto, R. A. Klemm, K. Kadowaki, "Applications using high-Tc superconducting terahertz emitters," *Sci. Rep.*, vol. 6, pp. 23178, 2016; doi: 10.1038/srep23178.
[92] T. Kashiwagi, K. Nakade, B. Marković, Y. Saiwai, H. Minami, T. Kitamura, C. Watanabe, K. Ishida, S. Sekimoto, K. Asanuma, T. Yasui, Y. Shibano, M. Tsujimoto, T. Yamamoto, J. Mirković, and K. Kadowaki, "Reflection type of terahertz imaging system using a high-Tc superconducting oscillator," *Appl. Phys. Lett.* vol. 104, pp. 022601, 2014.
[93] H. Sun, Z. Yang, N. V. Kinev, O. S. Kiselev, Y Lv, Y. Huang, L. Hao, X. Zhou, M. Ji, X. Tu, C. Zhang, J. Li, F. Rudau, R. Wieland, J. S. Hampp, O. Kizilaslan, D. Koelle, B. Jin, J. Chen, L. Kang, W. Xu, R. Kleiner, V. P. Koshelets, H. Wang, and P. Wu, "Terahertz spectroscopy of dilute gases using $Bi_2Sr_2CaCu_2O_{8+\delta}$ intrinsic Josephson junction stacks," *Phys. Rev. Applied*, vol. 8, pp. 054005. 2017.
[94] T. Kashiwagi, K. Nakade, Y. Saiwai, H. Minami, T. Kitamura, C. Watanabe, K. Ishida, S. Sekimoto, K. Asanuma, T. Yasui, Y. Shibano, M. Tsujimoto, T. Yamamoto, B. Marković, J. Mirković, R. A. Klemm, and K. Kadowaki, "Computed tomography image using subterahertz waves generated from a high-T_c superconducting intrinsic Josephson junction oscillator," *Appl. Phys. Lett.*, vol. 104, pp. 082603, 2014.
[95] M. Tsujimoto, T. Doi, G. Kuwano, A. Elarabi, I. Kakeya, "Engineering and characterization of a packaged high-T_c superconducting terahertz source module," *Supercond. Sci. Technol.* vol. 30, pp. 064001, 2017.
[96] Y. Simsek, V. Vlasko-Vlasov, A. E. Koshelev, T. Benseman, Y. Hao, I. Kesgin, H. Claus, J. Pearson, W.-K. Kwok and U. Welp, "Thick $Bi_2Sr_2CaCu_2O_{8+\delta}$ films grown by liquid-phase epitaxy for Josephson THz applications," *Supercond. Sci. Technol.* vol. 31, pp. 015009, 2018.
[97] S. Kalhor, M. Ghanaatshoar, T. Kashiwagi, K. Kadowaki, M. J. Kelly, and K. Delfanazari, "Thermal Tuning of High-T_c Superconducting $Bi_2Sr_2CaCu_2O_{8+\delta}$ Terahertz Metamaterial," *IEEE Photonics J*., vol. 9, no. 5, pp. 1–8, 2017.

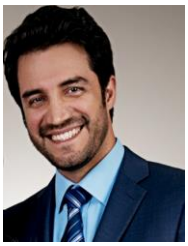

Kaveh Delfanazari (SM'18) is a Senior Research Associate in quantum technology at the University of Cambridge, UK. He received his PhD from the University of Tsukuba, Japan, where he investigated integrated high frequency devices and quantum emitters based on Josephson junctions. He was a Research Fellow and Project Leader, in superconducting and quantum metamaterials, at the Optoelectronic Research Centre (ORC), University of Southampton, UK, before joining the University of Cambridge.

Richard A. Klemm (M'10) received the Ph.D. in physics from Harvard University, Cambridge, MA, USA, in 1974. After a postdoctoral fellowship at Stanford University, CA, USA, he spent significant amounts of time at Iowa State University, Exxon Research and Engineering Company, and Argonne National Laboratory. He is now a Professor of Physics at the University of Central Florida, Orlando, FL, USA. Prior to entering graduate school, in 1970 he synthesized the first highly layered superconductor, $TaS_2(pyridine)_{1/2}$, in 1974 wrote his doctoral thesis, *Layered Superconductors*, on the theory of such materials, and is more recently the author of *Layered Superconductors Vol. 1* (Oxford University Press, 2012).

Hannah J. Joyce is a Reader in low-dimensional electronics at the University of Cambridge. She obtained her PhD in Physics from the Australian National University in 2010. She then joined the Department of Physics at the University of Oxford as a postdoctoral researcher. In 2013, Hannah joined the Department of Engineering at the University of Cambridge, where she leads a research group focusing on the development of nanomaterials for applications in photonics and electronics.

David A. Ritchie is Professor of Experimental Physics and a Fellow of Robinson College in Cambridge. He is also Professor of Semiconductor Science and Technology at Swansea University. He received his first degree, in physics, from the University of Oxford in 1980 and his D Phil from the University of Sussex in 1986 studying the physics of mixtures of liquid 3He and 4He at milli-kelvin temperatures. Since then he has been working on III-V semiconductor physics and has extensive experience of the growth, fabrication and measurement of low dimensional electronic and optical structures. He has been co-author of over 1100 papers and was awarded the 2008 Tabor medal and prize by the UK Institute of Physics for distinguished research in surface or nanoscale physics.

Kazuo Kadowaki (M'10) received the Ph.D. degree in physics from Osaka University, Japan, in 1980. He then worked as Postdoc at the Department of Physics, University of Alberta, AB, Canada (1982–1986), lecturer in Natuurkundig Laboratorium der Universiteit van Amsterdam, the Netherlands (1986–1990), group leader in National Research Institute for Metals, Japan (1990–1995), and Associate Professor (2005) and then Professor (2007-) of Institute of Materials Science, at the University of Tsukuba, Japan. He has discovered Kadowaki-Woods law in Solid State Physics and experimentally proved the Josephson plasma waves in layered superconducting BSCCO intrinsic Josephson junctions (IJJs) for the first time.